Journal of Building Engineering 91 (May 2024), 109701. https://doi.org/10.1016/j.jobe.2024.109701

The different effect of two paint systems on moisture buffer capacity of traditional and modern plasters

Alessandra Ranesi[1,2,*], Rosário Veiga[2], Paula Rodrigues[2], Paulina Faria[1].

1. CERIS, Dep. Civil Engineering, FCT, NOVA University Lisbon, 2829-516 Caparica, Portugal.

2. National Laboratory for Civil Engineering, Avenida do Brasil 101, 1700-066 Lisbon, Portugal

* corresponding author. e-mail address: a.ranesi@alumni.fct.unl.pt , tel: (+39) 3899975619, address: Avenida do Brasil, 101, 1700-066 Lisboa, Portugal.

e-mail address of each author: a.ranesi@alumni.fct.unl.pt, rveiga@lnec.pt, mprodrigues@lnec.pt, paulina.faria@fct.unl.pt

Abstract

Plasters can be finished with paint systems that can affect their moisture storage and transport properties. To confirm that, eight traditional and modern plastering mortars and pastes – based on cement, natural hydraulic lime, air lime, earth and gypsum - were coated with a vinyl paint (A) and an acrylic paint (B) and underwent the same hygroscopic characterization of the bare mortar samples. The effect of paint system A on water vapor adsorption and moisture buffering was small, in some cases positive. However, all the plasters painted with system A showed lower water vapor permeability than the bare plasters. The variation in the thickness of equivalent air layer was not the same for all the plastering mortars and pastes, suggesting that the different plastering substrates were still involved in the hygroscopic mechanism. The application of paint system B, instead, significantly reduced the hygroscopic behavior of the plasters, leveling their responses. The two paints, produced for different scopes and so with different kind and contents of constituents, have a diverse effect on those properties. Therefore, to optimize the passive contribution that plasters may have to indoor comfort, it is important to make a conscious choice when choosing paint finishing systems.

Keywords: coating, moisture buffer, water vapor permeability, vinyl paint, acrylic paint.

1. Introduction

The high amount (40%) of global energy consumed by the building sector (UNEP-SBCI, 2009) and the high amount (90%) of time people spend indoors (Frey et al., 2015) are two key factors to consider for indoors design. Coating materials can passively contribute to the indoor moisture control (Padfield 1999) diminishing the energy requirements of buildings (Zhang et al., 2017a; Osanyintola and Simonson 2006; Li and Ran 2023) and preventing risk of inhabitants' exposure to unhealthy environments and the possible development of chronic diseases (Arundel et al., 1986; Jones, 1999; Wolkoff, 2018; Fang et al., 1998; Guarnieri et al., 2023).

Among many coating materials, plastering mortars and pastes are commonly used to cover interior walls and ceilings. Thus, they have a large surface in contact with indoor air and their potential to contribute to passive moisture control can be important. Traditional and modern binder-based

plasters are found to have different moisture buffering properties (Ranesi et al., 2021a; Ranesi et al., 2021b). Plasters based on clay generally have a very high moisture capacity and for this reason their moisture behavior is often studied (Liuzzi et al., 2018; Randazzo et al., 2016, Ashour et al., 2011), but also other binder-based plasters have been the subject of interest in some research studies (Cascione at el., 2020; Santos et al., 2020, Ranesi et al., 2023), often in comparison with the clay-based ones.

Highly hygroscopic coating products are expected to adsorb and release moisture when the relative humidity (RH) increases or decreases, respectively (Posani et al., 2023; Gentile et al., 2023). The coatings passive moisture regulation can ensure better indoor air quality (IAQ). This can be particularly important especially under conditions of only natural ventilation, with little or no air exchanges, and high moisture production, like the case of a bedroom during the night occupied by two people sleeping (Rode et al., 2005). Furthermore, in indoor environments equipped with an HVAC system, a reduction of operational energy can be achieved through the moderation of RH peaks (Barbosa et al., 2020; Zhang et al., 2017b; Wargocki & Wyon, 2013) passively induced by highly hygroscopic coatings.

Nevertheless, it is common practice to apply a finishing layer (or more) on plasters. The reasons can be related to the vulnerability of some plasters to liquid water, particularly those based on clay or gypsum; their poor aesthetics, as is the case of plasters based on cement and natural hydraulic lime; usage habits; social factors; or simply the users' decision. Therefore, it seems reasonable to consider applying an additional finishing. Furthermore, although it is common to apply a layer of paint to mortars, both on interior and exterior walls, only a few papers analyze the effect of paints on the moisture properties of plastering mortars. In fact, most of the studies address the moisture transport and the drying capacity of the render-paint systems (Baltazar and Morais, 2023; Gonçalves et al., 2009; Brito et al., 2011), to better understand the degradation mechanisms that can be triggered in old buildings after a restoration work. Silicate, silicone, hydro-plioliteor acrylic paints for exterior walls and poly(vinyl acetate) paints for indoors are the modern representatives that have replaced traditional casein and lime-based paints. The composition of these modern waterborne paints is not known in detail, but in general they consist of a mixture of binders (resins), fillers, pigments and various additives, such as biocides, antifoam and freeze-thaw agents, plasticizers and thickeners, among others, designed to increase the performance and durability of the products (Novak and Ormsby, 2023).

Among all the possible paint finishing systems, the present study analyzes the application of two paints produced and commercialized, one for indoor and one for exterior use. The selected paints are both waterborne products formulated with a polyvinyl acetate resin (paint A) and an acrylic resin (paint B). The application of both paints on the different mortar substrates was made according to the same protocols and following the producers' recommendations and their influence on the hygroscopic behavior of mortars was evaluated.

2. Materials and Methods

2.1 The Commercial Paintings

- **PAINT A**

The paint (A) designed for indoor use was selected for the study. The paint was not yet on the market and a technical data sheet with its characteristics was not available; so, its laboratory characterization was carried out. The binder was identified by Fourier-transform infrared spectroscopy (FT-IR) after an extraction with chloroform. The results showed that the paint binder is a polyvinyl acetate resin (**Figure 1a**). The bulk density of the paint was determined by using a pycnometer and the non-volatile-matter content (NVMC) by drying at 105 °C in a ventilated oven for 1 hour (**Figure 2**).

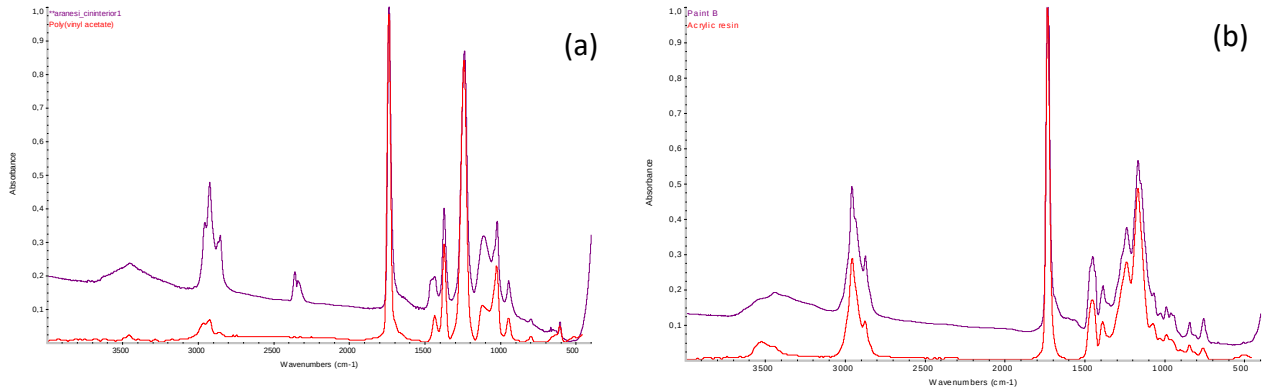

Figure 1. FT-IR spectra of: **(a)** binder of paint A (in purple) compared with a polyvinyl acetate (in red) from the literature; **(b)** binder of paint B (in purple) compared with an acrylic resin (in red) from the literature.

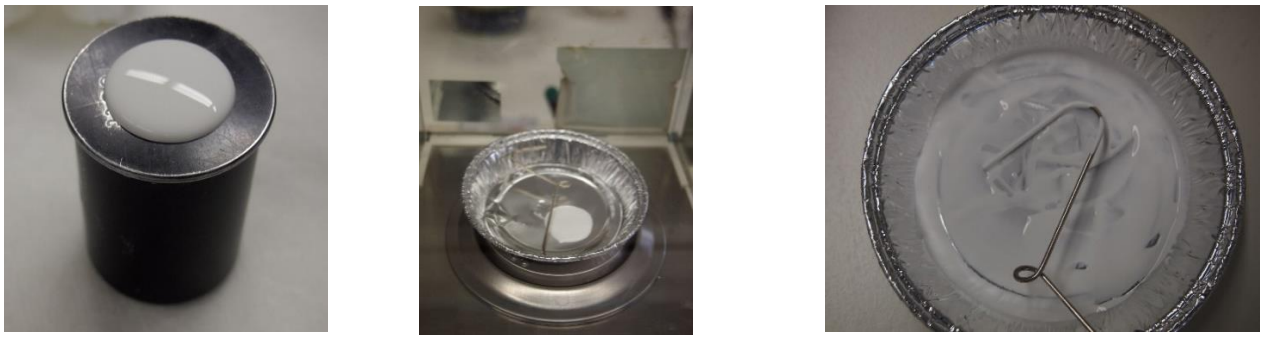

Figure 2. Laboratory assessment of bulk density and non-volatile-matter content of paint A.

The water vapor permeability (WVP) of the paint was tested on three specimens. The application was run on polytetrafluoroethylene sheets (PTFE or Teflon) (**Figure 3a**) in two layers, brushed with 24-hours drying interval and dried at 23 ± 2 °C e 50 ± 5 % RH for 30 days, in order to obtain a final dry thickness of about 140 µm.

(a) (b) (c) (d)

Figure 3. Application of the paint on Teflon **(a)**; disks cut **(b)**; disks sealed on water vapor permeability cups **(c)**; thickness of the dried paint system measurement **(d)**.

After drying, the paint films were detached from the PTFE sheet and cut into the shape of disks (approx. 80 mm diameter) (**Figure 3b**). Three film disks from the paint A were sealed with wax to the rims of the cups used for WVP tests (**Figure 3c**). A saturated solution of ammonium dihydrogen phosphate (300 ml) was used to obtain 93% RH environment inside the cups, based on EN ISO 7783 (2018). The circular test area of approx. 60 mm diameter was exposed to the test conditions inside a climatic chamber Aralab-Fitoclima 700 EDTU kept at 50 ± 5 % RH and 23 ± 2 °C until constant water vapor flux for at least five successive weighing intervals (24 hours). The determination of the films´ thicknesses was done by using an electronic micrometer according to EN ISO 2808 (2019). A value of 158 µm was found, by averaging eight measurements (**Figure 3d**). This real thickness value was considered for calculating the diffusion-equivalent air layer thickness (s_d) of 0.053 m that would correspond to the class V_1 – high water vapor transmission rate (s_d< 0.14 m) according to the standard (EN 1062-1, 2004) and is consistent with tabulated design values for paint emulsions referred in the standard ISO 10456 (2007).

- **Paint B**

A second commercial paint (B) designed for exterior surfaces was already characterized by the Portuguese National Laboratory for Civil Engineering (LNEC). It was used in the study to allow some comparison in terms of type of binder and water vapor properties, since exterior coatings are in general less permeable to water vapor than interior paints. Following the producer recommendations, it was applied in three layers to obtain around the same thickness as paint A. The FT-IR spectra of the binder B and the comparison and match with an acrylic resin from literature is shown in **Figure 1**b. The main characteristics found from the analysis of the paint A and obtained by the LNEC technical sheet for the paint B are synthetized in **Table 1**.

Table 1. Synthesis of the paints characterization.

	BD [g/mL]	NVMC [%]	s_d [m]	WVP class
Paint A	1.403	48.9	0.053	V_1
Paint B	1.373	52	>0.14 ;<1.4	V_2

Notation: BD – Bulk density; NVMC – Non-volatile-matter content; sd – Air layer thickness with equivalent diffusion; WVP – Water vapor permeability.

2.2 The Plastering Mortars

The products selected as substrates for the experimental campaign were five plastering mortars and three pastes used as plasters finishing layers (**Figure 4**). The plasters were elsewhere characterized at water vapor permeability and hygroscopic behavior (Ranesi et al., 2021a). The five mortars are based on different binders, namely: clayish earth (E), hydrated lime (AL), natural hydraulic lime (NHL) and cement (C), the latter produced with two different water:binder ratios (0.9 and 1.3). The pastes are based on calcium sulphate hemihydrate (G) and two combinations of the latter with hydrated lime (AL50_G50 and AL70_G20). For each product, three specimens of 40 mm x 40 mm x 20 mm approx. were used for the application of the paints. The apparent bulk density and open porosity of the plasters were obtained following EN 1936 (2006) by vacuum and hydrostatic weighing, except for the earth plasters which were geometrically determined as they would be damaged by water. **Table 2** presents a synthesis of the plasters and their characteristics, including their previous fresh state and hygroscopic characterization.

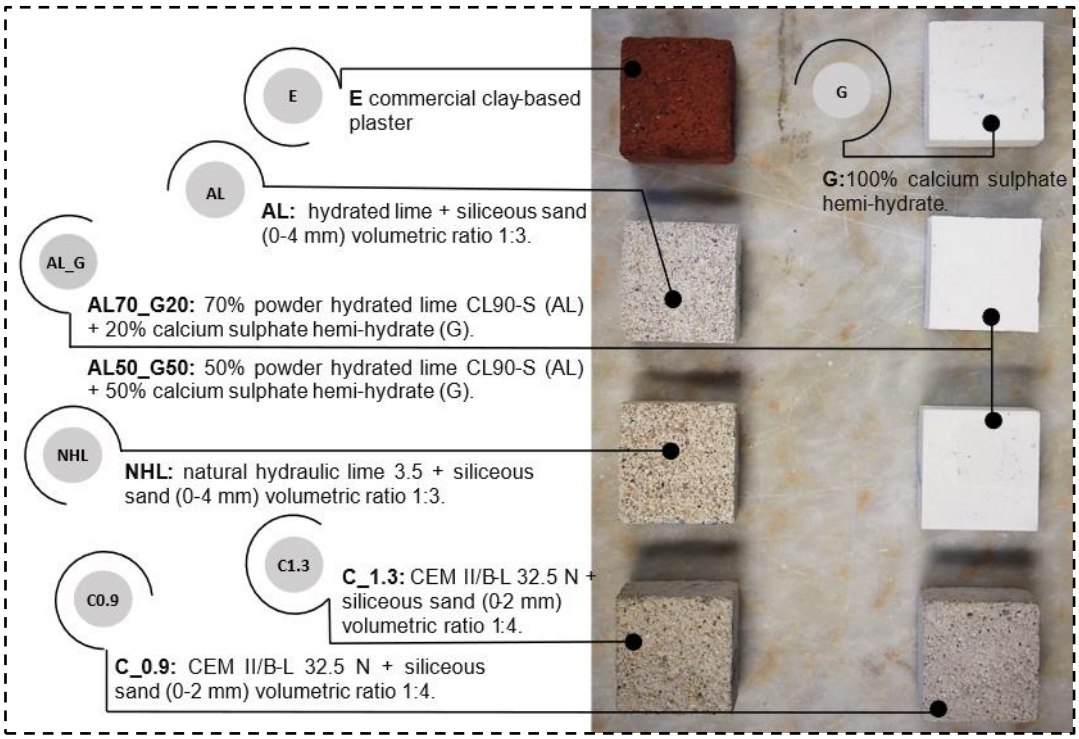

Figure 4. The plastering mortars and pastes ready for the application of the commercial paint system.

Table 2. Synthesis of characterization of the plastering mortars and finishing pastes selected as substrate for the study (Ranesi et al., 2021a).

Characterization	E	AL	NHL	C0.9	C1.3	G	AL50_G50	AL70_G20
Binder	Illitic Clay	CL90-S	NHL3.5	CEM II/B-L 32.5 N	CEM II/B-L 32.5 N	CSH	CSH + CL90-S	CSH + CL90-S
Aggregate type	Natural siliceous	Tagus river	Tagus river	Natural siliceous	Natural siliceous	-	-	Calcitic
Aggregate size [mm]	0-2	0-4	0-4	0-2	0-2	-	-	<45 µm

Water: binder [-]	0.2*	2.8	1.4	0.9	1.3	0.7	0.8	1
Fresh consistence [mm]	171±10	151±5	150±5	140±3	161±1	190±5	165±5	165±5
BD [kg/m^3]	1770	1755	1852	1937	1891	1048	1048	1043
OP [%]	-	27.4	25.6	20.4	23.3	46.3	50.7	53.4
μ [-]	9.07	7.43	9.32	20.42	14.48	5.49	5.22	5.18
MBV[g/(m^2%RH)]	1.49	0.42	0.80	0.84	0.82	0.61	1.03	1.27
MC_{12h} [g/m^2]	74.4	16.5	28.6	40.2	34.5	25.5	37.36	37.68

Notation: CL90-S -Hydrated air lime, NHL3.5- Natural hydraulic lime; CEM II/B-L 32.5 N - Cement; CSH – Calcium Sulphate Hemihydrate; * – Water/mix ratio; BD – Bulk density (dry); OP – Open porosity; μ – Water vapor resistance factor; MBV – Moisture buffering value by NORDTEST (Rode et al., 2005); MC_{12h} – Moisture content at 12 hours (DIN 18947, 2018).

The two commercial paint systems A and B were applied on the substrate specimens following the same procedure described for the application on PTFE sheets (intended dry thickness of about 140 μm in two layers for paint A and three layers for paint B, brushed with 24 hours drying interval and dried at 23 ± 2 ºC and 50 ± 5 % RH for 30 days). The number of paint layers applied on the mortars were selected according to the producer recommendations; nevertheless, the final dry thickness of design was kept the same.

2.3 Test Methods on the Painted Plasters

2.3.1 Water Vapor Permeability

After the application and drying of the paint A, as described in section **2.2**, three specimens of each mortar and paste were tested for water vapor permeability (WVP). This property quantifies the moisture transport capacity of the coatings that, combined with the moisture storage (quantified through the sorption isotherms), defines their moisture buffering properties. They were sealed with aluminum tape on the four lateral faces, to guarantee the mono-directionality of the water vapor flux, and with wax on the top of the cups containing calcium chloride, to ensure the ΔRH (0-50%) prescribed by the ISO 12572 (2016) for the dry cup conditions. The test procedure followed was the same described by Ranesi et al. (2021a) for the same, unpainted, specimens. Due to the shortage of specimens (the ones used in the study were mainly collected as leftover from other campaigns) it was not possible to perform the test of WVP for the mortars and pastes coated by the paint B system. Results were expressed as thickness of the equivalent air layer for the bare plasters and for the coated systems (paint A), at the experiment hygrothermal conditions (0% RH, 23 °C; 50% RH, 23 °C). The water vapor permeability of the air layer was calculated according to the Schirmer formula as prescribed by the ISO 12572 (2016).

2.3.2 Sorption Isotherms

After the WVP test, the sorption isotherms of the painted plasters were determined according to ISO 12571 (2013). The specimens were sealed with aluminum tape on their four lateral faces and on the base. Once dried in an oven at 45 °C until constant mass (mass variation lower than 0.1% in 24 hours, after three consecutive weighing), they were placed in the same climatic chamber used before, at 23 ± 5 °C and RH following the steps 30%, 50%, 70%, 80% and 95% RH, keeping each until steady state. The slope of the curves was used to calculate the specific moisture capacity for *middle humidity levels* (50-70% RH). During the test on the specimens with the application of the paint B

some technical issues prevented the climatic chamber from reaching the 95%. In order to show results compatible with the previous two tests, it was then decided to predict the curve based on a nonlinear regression analysis of the adsorption (0-80% RH) and the desorption (80%-0%RH) real data, available from the test.

The model selected has already been used by other authors (Ferreira et al., 2020) and is considered appropriate for simulating the response of hygroscopic materials. The equation (1) here applied, was firstly proposed by Hansen in 1986 (Hansen, 1986):

$$u = a \cdot (1 - \frac{\ln \varphi}{b})^{-\frac{1}{c}} \quad (\mathbf{1})$$

with u the moisture content [kg/kg], φ the relative humidity [-] and a, b, c the parameters to be calculated to fit the prediction curve to the experimental data. To fit the curve the most, it was decided to write two equations (one for adsorption and one for desorption) and calculate the R^2 for each segment (adsorption and desorption). The moisture content at 95% RH was successively predicted as the maximum value between the adsorption and the desorption equations applied at 95% RH. In **Table 3** a synthesis of the calculated parameters and R^2 is shown.

Table 3. Synthesis of the nonlinear regression analysis parameters: a, b, c and R^2 fitting the Hansen equation (Hansen, 1986) for adsorption and desorption.

Mortar	Adsorption			R^2	Desorption			R^2
	a	b	c		a	b	c	
E	0.006	24.742	0.024	0.99	0.006	0.724	0.827	0.98
AL	0.001	34.000	0.019	0.99	0.002	1.500	0.380	0.99
NHL	0.002	25.934	0.024	0.99	0.002	24.000	0.050	0.97
C1.3	0.003	28.249	0.026	0.99	0.002	0.926	1.271	0.98
C0.9	0.004	25.534	0.023	0.99	0.004	0.882	0.973	0.93
AL70_G20	0.004	26.569	0.024	0.99	0.005	23.913	0.059	0.98
AL50_G50	0.004	24.871	0.023	0.99	0.004	0.839	0.858	0.97
G	0.004	24.111	0.022	0.99	0.003	15.000	0.090	0.99

2.3.3 Moisture Penetration Depth

The moisture penetration depth (MPD) was calculated for bare mortars and for the systems mortars-paint A. The determination of this parameter for systems mortars-paint B was not possible due to the lack of experimental results regarding its WVP. The MPD represents the thickness of the material involved in the mechanism of moisture buffering. The higher the MPD of a plaster, the higher volume of material is involved in their moisture activity. Thus, it needs to be provided that the thickness of the plaster layer is greater than its MPD, to ensure that the plaster works at its maximum ideal moisture buffer capacity. Thus, to correctly determine the moisture buffering value of any building material, it is necessary to test specimens with thicknesses greater than the material's MPD. Two simplified methods of calculation for porous materials, present in literature (Rode et al., 2005; Woods et al., 2013), were followed.

The theoretical penetration depth calculated according to Rode (2005) as the "depth where the amplitude of moisture content variations is only 1% of the variation on the material surface", $d_{p,1\%}$, is given by equation (2):

$$d_{p.1\%} = 4.61\sqrt{\frac{D_w t_p}{\pi}} \quad (\mathbf{2})$$

being t_p the time in seconds of duration of the daily cycle 86400 s, and D_w the moisture diffusivity of the material depending on the water vapor permeability of the material (δ_p), its dry bulk density (ρ), its specific moisture capacity (ξ_u) and the saturation vapor pressure (p_s), defined by equation (3):

$$D_w = \frac{\delta_p p_s}{\rho \xi_u} \quad (\mathbf{3})$$

where ρ is the dry bulk density of the mortars (that was presented in section **2.2**), δ_p their water vapor permeability at ΔRH 0-50%, and $(\partial u/\partial \varphi)$ their specific moisture capacity according to the values of moisture content (u) at 50% RH and 70% RH. The saturation water pressure was calculated by equation (4):

$$p_s = 610.5\, e^{\frac{17.269\, t}{237.3+t}} \quad (\mathbf{4})$$

where t is the temperature [°C] of the experiment.

But, as observed by Maskell et al. (2018), the application of a model built for a semi-infinite or very thick material (as the one proposed by Rode et al. (2005)) may not be very suitable for plasters. Therefore, the model proposed by Woods et al., (2013) was also applied, considering 1/e (36.8% instead of 1%) as the ratio of the amplitude of moisture content variation (Maskell et al., 2018), and the theoretical penetration depth was calculated by equation (5):

$$d_{1/e} = \sqrt{\frac{D_w t_p}{\pi}} \quad (\mathbf{5})$$

2.3.4 Moisture Buffering Value

The practical moisture buffering value (MBV) is the quantification, under the selected standard conditions, of the moisture buffering capacity of a building material (plaster or system). Thus, the MBVs of the bare mortars and of the systems with paints A and B were experimentally obtained, even if tests were not simultaneously run. The specimens were sealed on their five faces with aluminum tape and preconditioned in a climatic chamber at 63 ± 5% RH and 23 ± 0.5 °C. A balance with 0.001 g resolution was used. The test was run according to the *middle humidity level* condition of the international standard ISO 24353 (2008). Thus, the specimens were exposed cyclically at two steps, 12 h each, of 75% and 50% RH, at the fixed temperature of 23 ± 0.5 °C and weighted after 3, 6, 9, 12 and 24 hours. The last three cycles out of five were considered for calculating the average value in adsorption and desorption of practical MBVs, according to the NORDTEST prescriptions (Rode et al., 2005).

Moreover, for comparison, the ideal MBV of bare and painted A mortars was calculated as proposed by Rode et al. (2005) by equation (6). The determination of this parameter for mortars with application of paint B was not possible due to lack of experimental results of WVP.

$$MBV_{ideal} = \frac{G_{(t)}}{\Delta RH} \quad (\mathbf{6})$$

In equation (6) ΔRH is the applied step in RH and $G_{(t)}$ the predicted moisture flux (uptaken and released), calculated by equation (7):

$$G_{(t)} = b_m \, \Delta_p \, h(\alpha) \sqrt{\frac{t_p}{\pi}} \quad (\mathbf{7})$$

being $\Delta_p = p_{s,50} - p_{s,0} = 1403.91$ Pa; b_m the moisture effusivity of the material. The moisture effusivity (b_m) is function of water vapor permeability (δ_p), dry bulk density (ρ), specific moisture capacity (ξ_u) and saturation water pressure (p_s) of the material, and was calculated by equation (8):

$$b_m = \sqrt{\frac{\delta_p \, \rho \, \xi_u}{p_s}} \quad (\mathbf{8})$$

were h(α) is a function of the fraction of the time-period where the RH is high (α). In the case of the present study, α was taken as ½ with h(α)=1.073 from equation (9):

$$h_{(\alpha)} \approx 2.252[\alpha(1-\alpha)]^{0.535} \quad (\mathbf{9})$$

turning the equation (5) for the predicted moisture flux for application of the cycle 12/24 prescribed by ISO 24353 (2008) into equation (10):

$$MBV_{(ideal)} = 0.00605 \, b_m \Delta_p \sqrt{t_p} \quad (\mathbf{10})$$

Thus, the ideal MBV of the unpainted and painted (A) mortars will mostly depend on their moisture effusivity (b_m), meaning that, under the same testing conditions, differences of results will mainly rely on materials water vapor permeability and moisture capacity.

3. Results and Discussion

3.1 Water Vapor Permeability

An overall increase is observed in the air layer thickness with equivalent water vapor diffusion of the plastering mortars and pastes, introduced by the application of the paint A (**Figure 5**). The effect of paint A is more evident for the gypsum pastes (AL70_G20, AL50_G50, G) probably due to the higher permeability of the pastes.

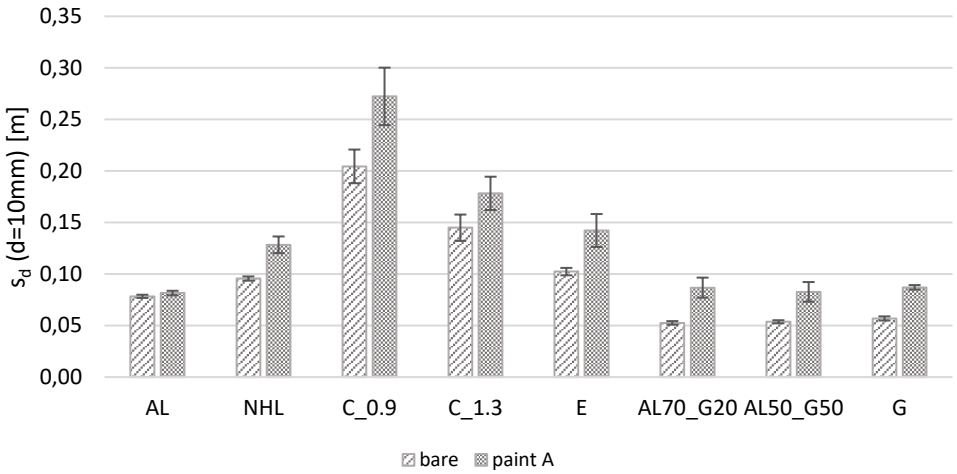

Figure 5. Thickness of the equivalent air layer (s_d) of the plasters with and without paint A application (average and standard deviation).

Ramos *et al.* (2010) also tested gypsum and gypsum-lime (50%-50%) finishing plasters coated by 50 µm layers of both vinyl and acrylic paints. The authors observed that the water vapor resistance introduced by the paints is influenced by the base material, consistent with the results found here. Indeed, the different influence of the same paint on plastering mortars and pastes can also be related to their different surface properties, like the surface roughness and compactness, that can lead to a different final dried thickness of the paint film. The effect of the application of the acrylic paint B on the studied mortars was not analyzed, but it seems relevant to refer that in literature (Baltazar and Morais, 2023) it was found that the presence of acrylic paint layer results in the decrease of the water vapor diffusivity of systems made of mortars based on natural hydraulic lime, on cement and on air lime.

3.2 Sorption Isotherms

Sorption isotherms of the bare mortars (dashed black line), the vinyl painted system A (continuous grey line), the acrylic painted system B (only symbols, blue) and the predicted response of the painted system B (continuous blue line) are shown in **Figure 6**, with y axes differently scaled, according to the system plaster-paint maximum moisture content, for a better reading of results**.** The expression of moisture content [%] is given as mass by mass ($u=(m_i–m_0)/m_0$) with m_i being the i-th mass and m_0 de initial dry mass of the specimens. It is observed a difference between the application of the two paints, with acrylic paint B generally reducing the moisture capacity of the systems, mainly for mortars that would show a hysteresis at high RH levels. The application of the vinyl paint A, instead, overall does not modify the systems adsorptions. These results are consistent with the findings on water vapor resistance of the systems and the water vapor permeability classes declared by the producers.

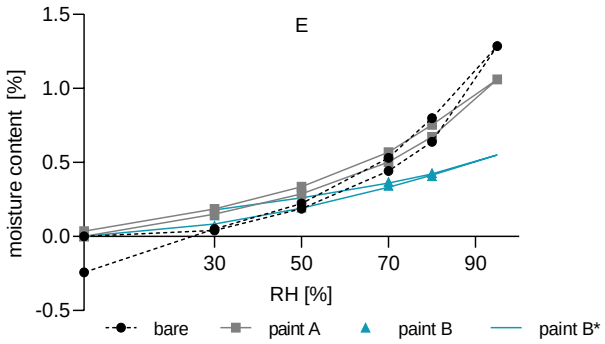
E
moisture content [%]
1.5
1.0
0.5
0.0
-0.5
30
50
70
90
RH [%]
bare
paint A
paint B
paint B*

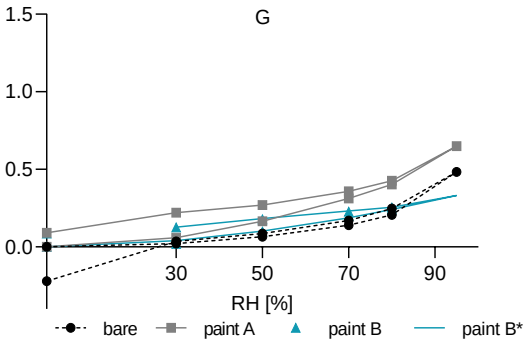
G
1.5
1.0
0.5
0.0
30
50
70
90
RH [%]
bare
paint A
paint B
paint B*

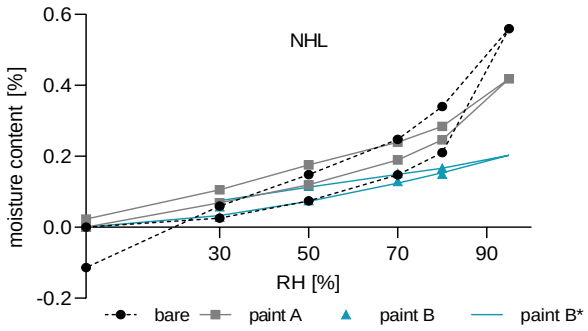
NHL
moisture content [%]
0.6
0.4
0.2
0.0
-0.2
30
50
70
90
RH [%]
bare
paint A
paint B
paint B*

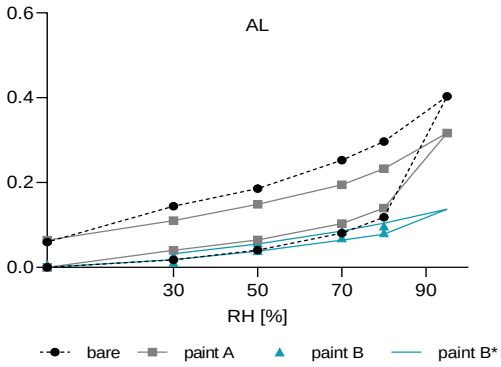
AL
0.6
0.4
0.2
0.0
30
50
70
90
RH [%]
bare
paint A
paint B
paint B*

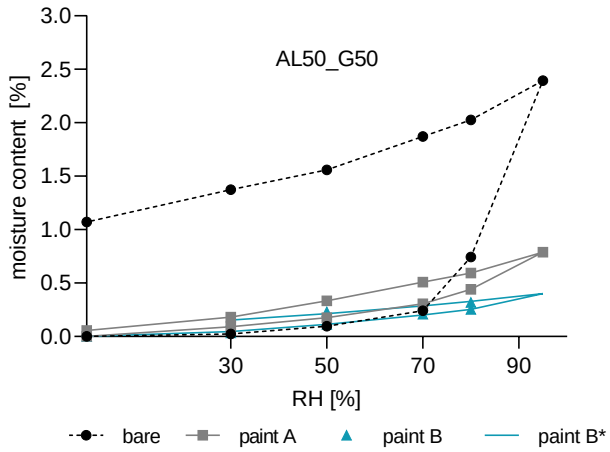
AL50_G50
moisture content [%]
3.0
2.5
2.0
1.5
1.0
0.5
0.0
30
50
70
90
RH [%]
bare
paint A
paint B
paint B*

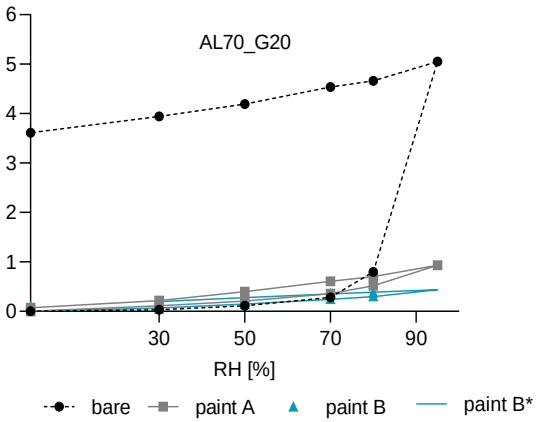
AL70_G20
6
5
4
3
2
1
0
30
50
70
90
RH [%]
bare
paint A
paint B
paint B*

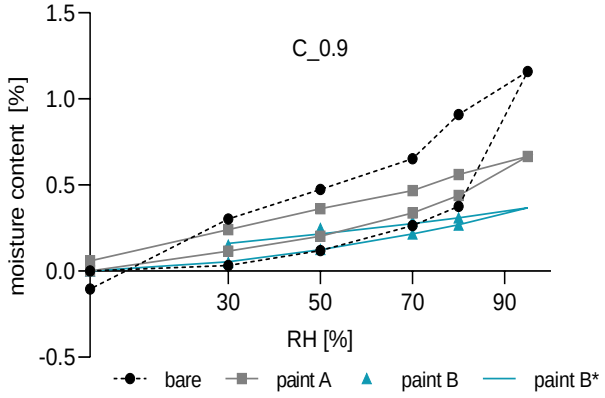
C_0.9
moisture content [%]
1.5
1.0
0.5
0.0
-0.5
30
50
70
90
RH [%]
bare
paint A
paint B
paint B*

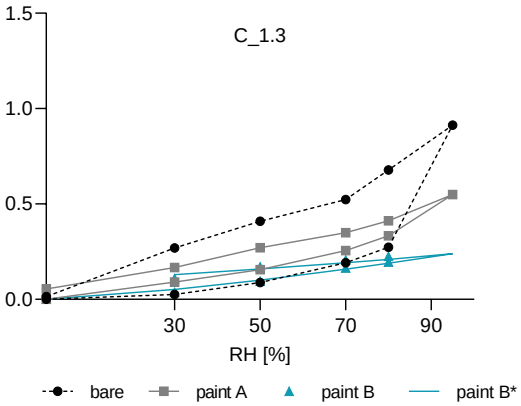
C_1.3
1.5
1.0
0.5
0.0
30
50
70
90
RH [%]
bare
paint A
paint B
paint B*

Figure 6. Sorption isotherms 0% -95% RH. In black (dashed) the bare mortars, in grey (continuous) the plasters + paint A, in blue (only symbols) the plasters + paint B and in blue (continuous) the predicted curves for plasters + paint B (*).

When the vinyl paint A is applied on mortars G, NHL, C_0.9 and E the adsorption curves observed are slightly higher than the ones of the bare mortars. However, these bare mortars were all showing a negative moisture content when dried at the end of the test. It is possible that these mortars, and mortar E, were not completely dried when the test started, so the m_0 accounted for calculation is higher than the real dry mass (final one). Nevertheless, the test was performed according to the standard (ISO ISO12571, 2013) and the specimens reached equilibrium (dry) before being moved to the climatic chamber to start the RH steps. The corrected curve (using the final dried mass as m_0) is presented in **Figure 7** and shows that the application of vinyl paint A, as expected, did not increase the moisture adsorption.

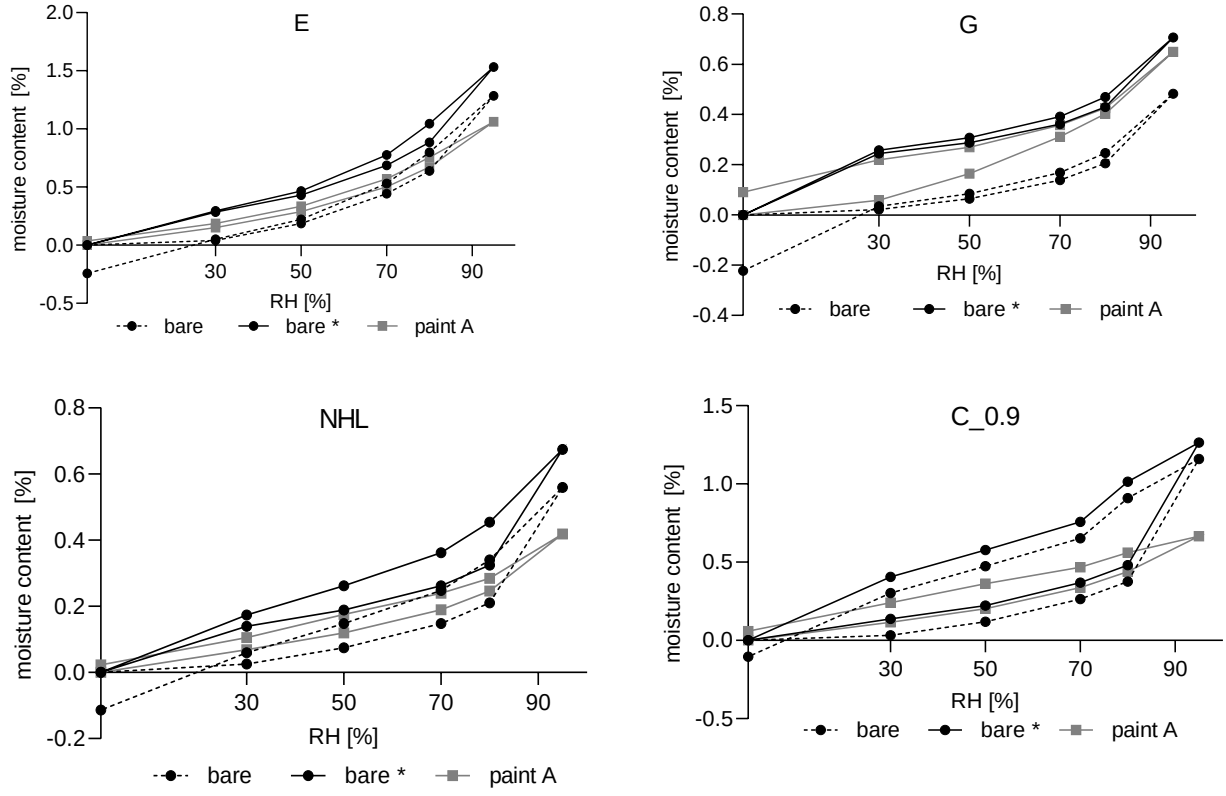

Figure 7. Correction factor (*) applied on the sorption isotherms for mortars based on: E – earth, G – gypsum, NHL – Natural Hydraulic Lime, C_0.9 – cement.

Nevertheless, the slope of the curves of the painted and unpainted specimens, needed for the calculation of the moisture penetration depth and the theoretical MBV, resulted similar.

3.3 Moisture Penetration Depth

The moisture diffusivity (D_w) of the plasters was calculated according to equation (3). The saturation vapor pressure calculated according to equation (4) at the temperature of 23°C was found to be equal to 2807.81 Pa. The moisture storage capacity (ξ_u) was obtained from the sorption curve although, as evidenced by McGregor et al. (2014) and by Roels and Janssen (2006), the non-linearity of the hygric properties represents a challenge for the determination. The same authors (McGregor et al., 2014; Roeals and Janssen, 2004) suggest considering the middle range of RH, excluding the

sharpest segments of the slopes. Thus, the range of RH 50-70% of the sorption curves was considered to calculate the moisture storage capacity of each plaster, also consistent with the moisture buffering testing conditions selected with the RH step 50-75%. Results (**Table 4**) of moisture penetration depth for the bare clay plaster for $d_{p,1\%}$ and $d_{p,1/e}$ are 37 mm and 8 mm, respectively, for a calculated diffusivity of 2.379 E^{-9} m^2/s. A similar result was found by Maskell et al. (2018) for an earthen plaster, with calculated moisture penetration depth at 1% and 1/e, respectively 57 mm and 12 mm. When the vinyl paint A is applied, the moisture diffusivity decreases, and the thickness of the equivalent air layer of the system increases. The diffusivity when the clay plaster is painted, in fact, decreases to 2.0521 E^{-9} m^2/s and the penetration depth, according to one model or the other, is found to be equal to 35 mm and 8 mm.

Table 4. Synthesis of results for calculated moisture penetration depth of the bare and with paint A mortars.

Plaster	**d_{real}**	**D_w [m^2/s]**		**$d_{p,1\%}$** [mm]		**$d_{p,1/e}$** [mm]	
	[mm]	Bare	Paint A	Bare	Paint A	Bare	Paint A
E	22	2.379E-09	2.051 E-09	37	35	8	8
AL	23	1.993 E-08	2.001 E-08	108	108	23	23
NHL	20	8.442 E-09	6.625 E-09	70	62	15	13
C1.3	21	3.865 E-09	2.425 E-09	48	38	10	8
C0.9	22	1.895 E-09	2.108 E-09	33	35	7	8
AL70_G20	21	1.161 E-08	7.983 E-09	82	68	18	15
AL50_G50	22	1.331 E-08	9.674 E-09	88	75	19	16
G	21	2.488 E-08	8.170 E-09	121	69	26	15

Notation: D_w – moisture diffusivity (m^2/s); $d_{p,1\%}$ and $d_{p,1/e}$ – moisture penetration depth (mm); binders: E – earth; AL – air lime; NHL – natural hydraulic lime; C – cement; G – gypsum.

It is evident that, according to both models, the decrease in MPD of the mortars with the application of paint A is very small, probably having little or no consequences on their moisture buffering capacity. In case the d_p=1% method is followed, all the tested specimens are thinner than their calculated MPD (all the section is involved in the mechanism either with or without paint). In that case, their practical MBV would be an underestimation of the ideal MBV. If the MPD is, instead, lower than the real thickness of the specimens (according to $d_{p,1/e}$ calculations) then the practical MBV of mortars - vinyl paint systems would be lower than the ideal MBV of bare mortars for NHL, C1.3, Al70_G20, AL50_G50, G, greater for C_0.9 and a perfect match for E and AL.

3.4 Moisture Buffering Value

MBV resulting from the experimental campaign of bare, painted A and painted B plasters are shown in **Figure 8** with the limits proposed by NORDTEST (Rode et al., 2005) for building materials. The mortars AL, NHL and C_0.9 showed an MBV slightly higher than *limited* both with and without the application of the paint A. The MBVs of C_1.3 and G are very similar and between the *limited* and *moderate* classifications. The application of paint A slightly increases their buffering capacity. The same effect is visible on the gypsum pastes AL70_G20 and AL50_G20, even if for higher values (very close to the *good* class). The *good* moisture buffering of the clay-based plaster (with the highest MBV equal to 1.41 $g \cdot m^{-2}\%RH^{-1}$), instead, is slightly reduced by the paint A application. Overall, paint system A does not seem to have a big impact on the moisture buffering of the mortars. Paint system B, instead, developed for outdoors use with higher water vapor resistance reduces the

performances in all cases, seeming to equalize all the mortars to *negligible,* in some case *low limited* class and limiting, thus, their moisture buffer capacity.

The slight increase in moisture content of the system with application of the vinyl paint A, was further investigated. The possibility of the moisture capacity of the paint itself was tested through ISO 24353 (2008). For the scope, three applications of the vinyl paint A on sheet glass were prepared and their moisture buffering capacity was evaluated. The MBV (calculated according to Rode at al., 2005) was found 0.06 ± 0.013 g/ (m^2·RH%) which shows a small hygroscopic response of the paint itself. This little moisture storage capacity of the vinyl paint A probably contributed to the adsorption and desorption capacity of the system.

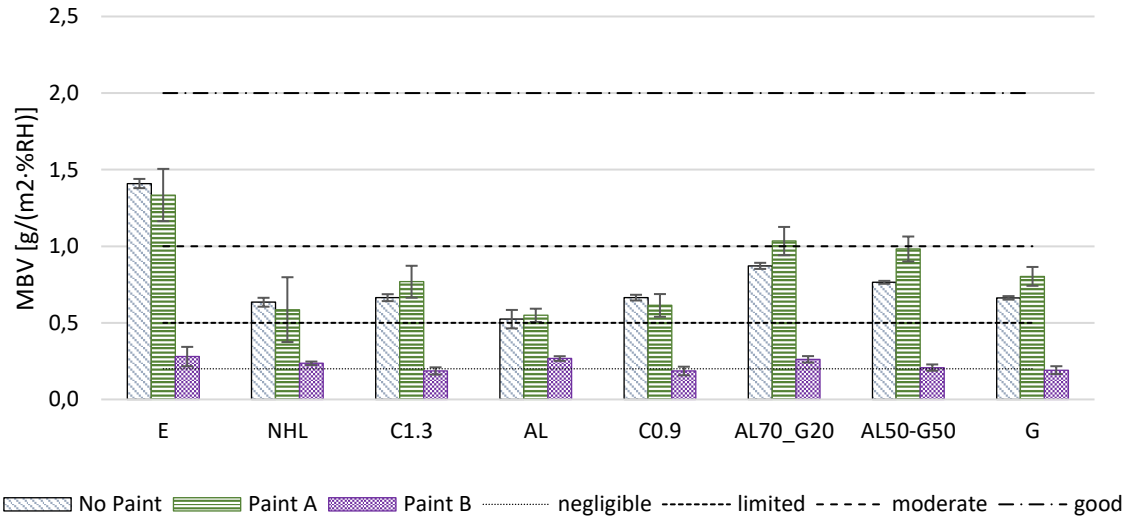

Figure 8. MBV of the plasters with and without paints (average and standard deviation) compared with limits of classes from NORDTEST (Rode et. Al, 2005).

The ideal MBV for the bare mortars and the system mortars with paint A was calculated according to equation (10). The same parameters described for the calculation of moisture penetration depth (section **3.3**) were used. Results of practical and ideal MBV (in this case only for plasters with paint A) are resumed in **Table 5**.

Table 5. Synthesis of the ideal and practical MBV according to ISO 24353 (2018) of the plasters.

Plaster	**No Paint**		**Paint A**		**Paint B**
	MBV_{ideal}	$MBV_{practical}$	MBV_{ideal}	$MBV_{practical}$	$MBV_{practical}$
E	1.95	**1.41**	1.53	**1.33**	**0.28**
AL	0.88	**0.52**	0.85	**0.55**	**0.27**
NHL	1.11	**0.63**	0.94	**0.59**	**0.24**
C1.3	1.08	**0.66**	0.96	**0.77**	**0.19**
C0.9	1.10	**0.66**	0.92	**0.61**	**0.19**
AL70_G20	1.72	**0.87**	1.27	**1.03**	**0.26**
AL50_G50	1.58	**0.76**	1.21	**0.98**	**0.21**
G	1.09	**0.66**	1.24	**0.80**	**0.19**

In both cases (bare and vinyl painted mortars) the practical MBV is lower than the ideal MBV. This can be related to the assumptions made by the equation (6) for the calculation of the theoretical MBV, as observed by Roels and Janssen (2006), of a moisture behavior related to the square root of time when the surface film resistance is neglected, and the specimen is assumed semi-infinite. Moreover, according to results of MPD with d_p=1%, it is possible that the real thickness of the specimens is lower than the ideal thickness involved in the mechanism. The fact that the ideal value is found always to overestimate the real behavior of the material and that probably there are other factors affecting the moisture buffering behavior was concluded also by Maskell et al. (2018). Nevertheless, the differences between the adsorption and desorption curves of the painted (A) and unpainted specimens are very small, as showed in **Figure 9**. Considering that the tests were not run simultaneously, it seems reasonable to conclude that the application of the vinyl paint A did not strongly modify the MBV of the plasters. It seems possible, in some cases like the air lime-based mortar (AL), that the paint system contributed to a faster stabilization at the quasi-steady state. Instead, the acrylic paint system B, with lower water vapor permeability, has a very big impact on the moisture buffer capacity of these mortars, lowering very much their response also when tested at quasi-steady states.

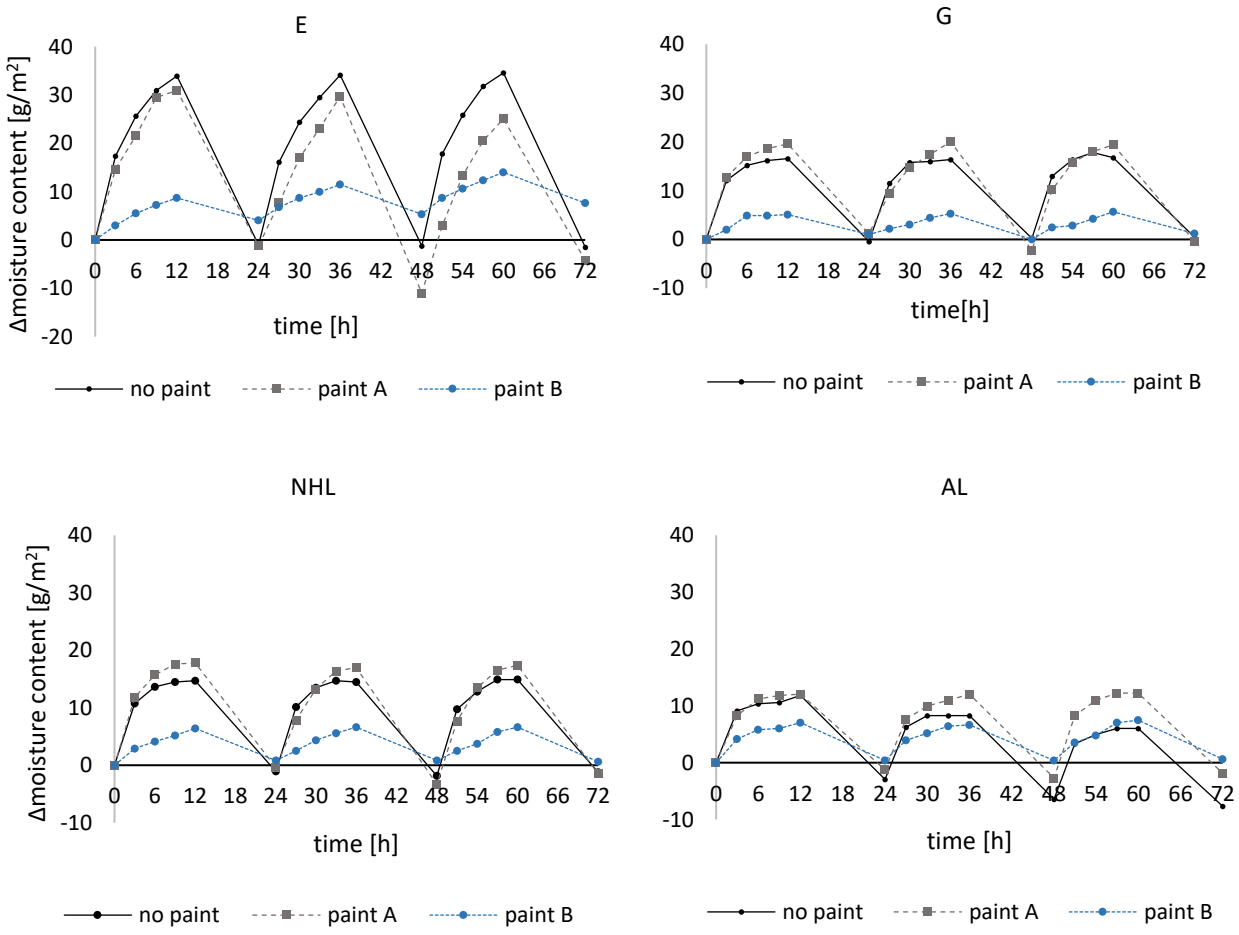

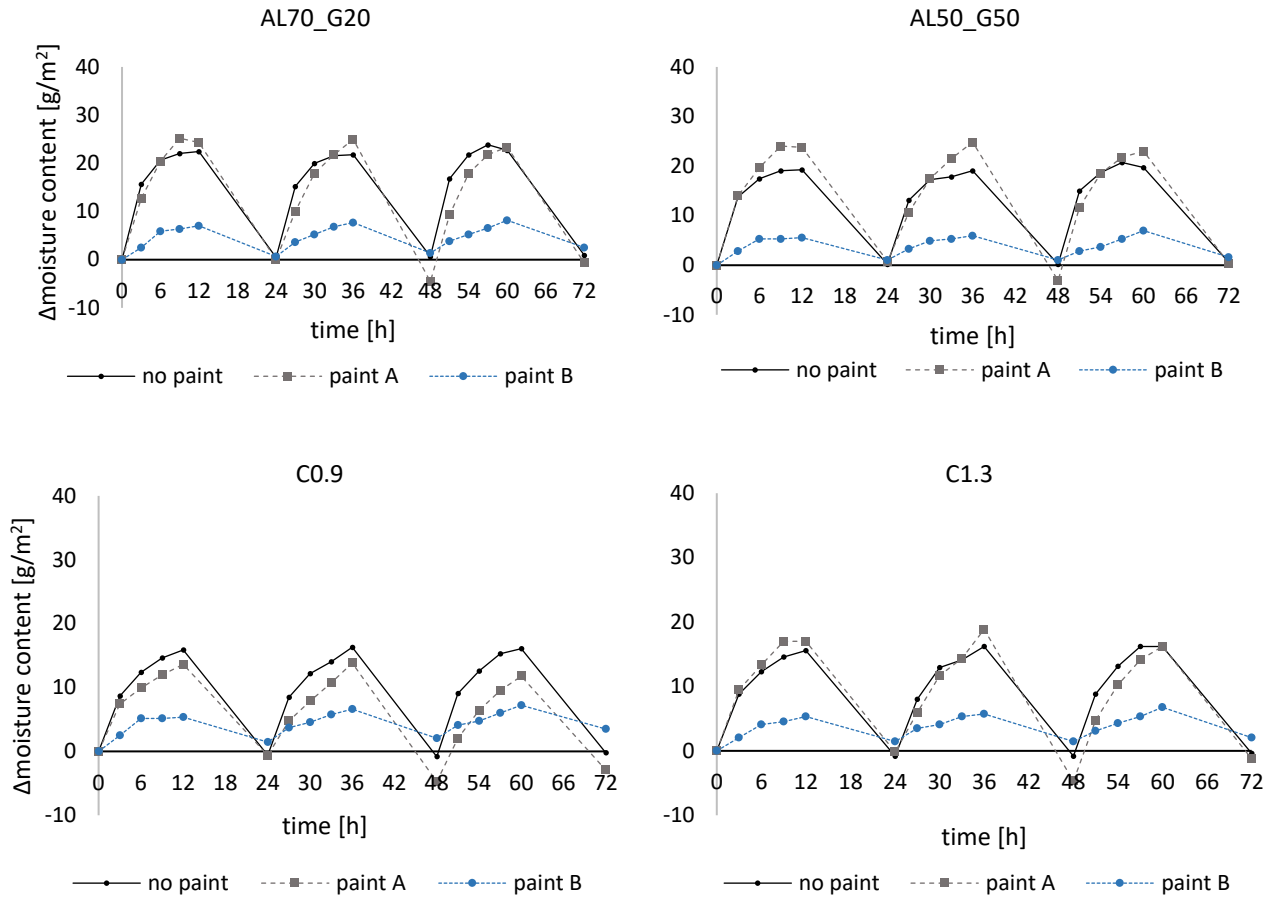

Figure 9. Adsorption/desorption curves of the last three cycles run in *middle humidity level* according to ISO 24353 (2008) over the time (hours). In blue (dashed) the painted A, in grey (dashed) the painted B and in black (continuous) the unpainted specimens.

4. Conclusions

The present study shows that two different waterborne emulsion paints based on polyvinyl acetate binder (A) and acrylic binder (B) have very different effects on moisture buffer properties of the plastering mortars they are applied on. The vinyl paint has very small effects while the acrylic paint significantly reduces the moisture capacity of the systems. Overall:

- The thickness of the equivalent air layer of the tested traditional and modern plastering mortars was increased by the vinyl paint A application showing more effect on some plasters than on others. Namely, the highest effect was observed for the pastes of gypsum and gypsum - air lime (G, AL70_G20, AL50_G50). These bare pastes have the highest WVP and the lowest surface roughness. All the other systems, apart from the air lime-based mortar- vinyl paint A, showed a lower permeability to water vapor by the application of the vinyl paint.
- The application of the vinyl paint had no significative effect on the sorption isotherms of the plasters, with equilibrium reached at a moisture content very similar to that of their unpainted versions. The application of acrylic paint B, instead, decreased the equilibrium moisture content at all the RH steps. Recalling that the acrylic paint was developed for outdoors application with lower water vapor permeability, results point out a correlation between water vapor diffusivity of the system and moisture storage.

- The moisture penetration depth (MPD) was calculated for bare plasters and plasters with the application of the vinyl paint according to two different methods (1% and 1/e). The MPDs calculated are quite different, with the results from the 1% method always above the real thickness of the specimens, and the results from the 1/e method almost always below or equal to it. However, according to both calculation methods, the MPD of the plasters is only slightly reduced by the paint A application.
- The practical MBV results confirm the different effects of the two paints, with the very small influence of vinyl paint A on the moisture buffering of plasters and the large reduction of the buffering capacity introduced by acrylic paint B. The ideal MBV is always an overestimation of the real MBV, as already observed by other authors, probably because it is modelled on specimens with thicker penetration depths ($d_{p,1\%}$) or specimens assumed as semi-infinites, for instance.

Finally, with the present knowledge, it seems difficult to determine in advance if a paint system would significantly affect the moisture buffering of plastering mortars and pastes without characterizing the moisture buffering properties and capacity of the specific system (plaster + paint). The water vapor permeability of the paint can have an important effect for the moisture diffusion and storage of the system. Moreover, the present work leaves aside all the application-related-condition, such as the substrate of application, the ratio between the volume of the room and the surfaces coated, the use of the room, the ventilation rate. These conditions are needed to fully quantify the environmental effect that the application of the studied coatings might have. Nevertheless, according to the results obtained in the present work, it seems possible to conclude that more recent indoor paints have been optimized to avoid jeopardizing the potential passive moisture buffering activity of the system plaster-paint.

Acknowledges

This research was supported by Portuguese Foundation for Science and Technology (FCT- Fundação para a Ciência e a Tecnologia): PD/BD/150399/2019 – 1st author Doctoral Training Program EcoCoRe. The authors are also grateful for FCT support through funding UIDB/04625/2020 of the research unit CERIS (DOI: 10.54499/UIDB/04625/2020). The authors would like to thank the National Laboratory for Civil Engineering of Portugal (LNEC) for the laboratory equipment and the support provided through the projects REuSE - Wall coverings for Rehabilitation: Safety and Sustainability and RevBar – Polymeric based barrier coatings: functionality and sustainability.

References

Arundel AV, Sterling EM, Biggin JH, Sterling TD. Indirect health effects of relative humidity in indoor environments. Environmental Health Perspectives. 1986; 65: 351-61.

Ashour T, Georg H, Wu W. An experimental investigation on equilibrium moisture content of earth plaster with natural reinforcement fibres for straw bale buildings. Applied Thermal Engineering. 2011; 31(2–3): 293-303. https://doi.org/10.1016/j.applthermaleng.2010.09.009

Barbosa F C, de Freitas V P, Almeida M. School building experimental characterization in Mediterranean climate regarding comfort, indoor air quality and energy consumption. Energy and Buildings. 2020; 212: 109782. https://doi.org/10.1016/j.enbuild.2020.109782

Baltazar L G, Morais A. Assessment of the Type of Paint on Performance of Rendering Mortars. CivilEng. 2023; 4: 454–468. https://doi.org/10.3390/civileng4020026

Brito V, Gonçalves T D, Faria P. Coatings applied on damp building substrates: Performance and influence on moisture transport. Journal of Coatings Technology and Research. 2011; 8: 513–525. https://doi.org/10.1007/s11998-010-9319-5

Cascione V, Maskell D, Shea A, Walker P, Mani M. Comparison of moisture buffering properties of plasters in full scale simulations and laboratory testing. Construction and Building Materials. 2020; 252: 119033. https://doi.org/10.1016/j.conbuildmat.2020.119033

EN 1062-1:2004. Paints and varnishes - Coating materials and coating systems for exterior masonry and concrete - Part 1: Classification. CEN, Brussels, Belgium.

EN 1936: 2006. Natural stone test methods - Determination of real density and apparent density, and of total and open porosity. CEN, Brussels, Belgium.

Fang L, Clausen G, Fanger P O. Impact of temperature and humidity on the perception of indoor air quality. Indoor Air. 1998; 8: 80-90. DOI: 10.1111/j.1600-0668.1998.t01-2-00003.x

Ferreira C, de Freitas V P, Delgado J M P Q. The influence of hygroscopic materials on the fluctuation of relative humidity in museums located in historical buildings. Studies in Conservation. 2020; 65(3): 127-141. https://doi.org/10.1080/00393630.2019.1638666

Frey S E, Destaillats H, Cohn S, Ahrentzen S, Fraser MP. The effects of an energy efficiency retrofit on indoor air quality. Indoor Air. 2015; 25: 210-219. https://doi.org/10.1111/ina.12134

Gentile V, Libralato M, Fantucci S, Shtrepi L, Autretto G. Enhancement of the hygroscopic and acoustic properties of indoor plasters with a Super Adsorbent Calcium Alginate BioPolymer. Journal of Building Engineering. 2023; 76: 107147. https://doi.org/10.1016/j.jobe.2023.107147

Gonçalves T D, Pel L, Rodrigues J D. Influence of paints on drying and salt distribution processes in porous building materials. Construction and Building Materials. 2009; 23: 1751-59. doi: 10.1016/j.conbuildmat.2008.08.006

Guarnieri G, Olivieri B, Senna G, Vianello A. Relative humidity and its impact on the immune system and infections. International Journal of Molecular Sciences. 2023; 24(11):9456. https://doi.org/10.3390/ijms24119456

Hansen K K. Sorption Isotherms: A Catalogue. Technical Report 162/86. Technical University of Denmark (Eds). 1986.

ISO 10456: 2007. Building materials and products Hygrothermal properties — Tabulated design values and procedures for determining declared and design thermal values. ISO, Geneva,

Switzerland.

ISO 12571: 2013. Hygrothermal performance of building materials and products — determination of hygroscopic sorption properties. ISO, Geneva, Switzerland.

ISO 12572:2016. Hygrothermal performance of building materials and products — Determination of water vapour transmission properties — Cup method. ISO, Geneva, Switzerland.

ISO 7783: 2018. Paints and varnishes - Determination of water-vapour transmission method – cup method. ISO, Geneva, Switzerland.

ISO 2808: 2019. Paints and varnishes — Determination of film thickness. ISO, Geneva, Switzerland.

ISO 24353: 2008. Hygrothermal performance of building materials and products - Determination of moisture adsorption/desorption properties in response to humidity variation. ISO, Geneva, Switzerland.

Jones AP. Indoor air quality and health. Atmospheric Environment. 1999; *33*: 4535–4564. https://doi.org/10.1016/S1352-2310(99)00272-1

Li X, Ran M. Gypsum-based humidity-control material: preparation, performance and its impact on building energy consumption. Materials. 2023; 16:5211. https://doi.org/10.3390/ma16155211

Liuzzi S, Rubino C, Stefanizzi P, Petrella A, Boghetich A, Casavola C, Pappalettera G. Hygrothermal properties of clayey plasters with olive fibers. Construction and Building Materials.2018; 158: 4-32. https://doi.org/10.1016/j.conbuildmat.2017.10.013

McGregor F, Heath A, Fodde E, Shea A. Conditions affecting the moisture buffering measurement performed on compressed earth blocks. Building and Environment. 2014; 75: 11-18. DOI: 10.1016/j.buildenv.2014.01.009

Maskell D, Thomson A, Walker P, Lemke M. Determination of optimal plaster thickness for moisture buffering of indoor air. Building and Environment. 2018; 130: 143–150. DOI: 10.1016/j.buildenv.2017.11.045

Novak M, Ormsby B. Poly(Vinyl Acetate) Paints: A Literature Review of Material Properties, Ageing Characteristics, and Conservation Challenges. Polymers. 2023; 15: 4348. https://doi.org/10.3390/polym15224348

Osanyintola OF, Simonson CJ. Moisture buffering capacity of hygroscopic building materials: Experimental facilities and energy impact. Energy and Buildings. 2006; 38: 1270–1282. DOI: 10.1016/j.enbuild.2006.03.026

Padfield T. Humidity buffering of the indoor climate by absorbent walls. In 5th Symposium on Building Physics in the Nordic Countries, 2, 637–644. 1999.

Pederneiras C, Veiga R, de Brito J. Rendering mortars reinforced with natural sheep's wool fibers. Materials. 2019; 12: 3648. DOI: 628 10.3390/ma12223648

Posani M, Voney V, Odaglia P, Brumaud C, Dillenburger B, Habert G. Re-thinking Indoor Humidity Control Strategies: The potential of additive manufacturing with low-carbon, super hygroscopic materials. (Under revision in Nature Communications, from November 2023). https://doi.org/10.21203/rs.3.rs-3427939/v1

Ramos NMM, Delgado JMPQ, de Freitas VP. Influence of finishing coatings on hygroscopic moisture buffering in building elements. Construction and Building Materials. 2010; 24: 2590–2597. DOI: 10.1016/j.conbuildmat.2010.05.017

Randazzo L, Montana G, Hein A, Castiglia A, Rodonò G, Donato DI. Moisture absorption, thermal conductivity and noise mitigation of clay based plasters: The influence of mineralogical and textural characteristics. Applied Clay Science. 2016; 132–133: 498-507. https://doi.org/10.1016/j.clay.2016.07.021

Ranesi A, Veiga R, Faria P. Traditional and Modern Plasters for Built Heritage: Suitability and Contribution for Passive Relative Humidity Regulation. Heritage. 2021a; 4: 2337–2355. DOI: 10.3390/heritage4030132

Ranesi A, Faria P, Veiga R. Laboratory characterization of relative humidity dependant properties for plasters: a systematic review. Construction and Building Materials. 2021b; 304: 124595. https://doi.org/10.1016/j.conbuildmat.2021.124595

Ranesi A, Faria P, Freire M T, Gonçalves M, Veiga R. Gypsum plastering mortars with acacia dealbata biowaste additions: Effect of different fractions and contents on the relative humidity dependent properties. Construction and Building Materials. 2023; 404:133283. ISSN 0950-0618. https://doi.org/10.1016/j.conbuildmat.2023.133283

Rode C, Peuhkuri RH, Mortensen LH, Hansen KK, Time B, Gustavsen A, Ojanen T, Ahonen J, Svennberg K, Harderup LE, Arfvidsson J. Moisture buffering of building materials. Technical University of Denmark, Department of Civil Engineering. BYG Report, R-127. 2005.

Roels S, Janssen H. A comparison of the Nordtest and Japanese test methods for the moisture buffering performance of building materials. Journal of Building Physics. 2006; 30:137. DOI: 10.1177/174425910606810

Santos T, Gomes M I, Santos Silva A, Ferraz E, Faria P. Comparison of mineralogical, mechanical and hygroscopic characteristic of earthen, gypsum and cement-based plasters. Construction and Building Materials. 2020; 254: 119222. https://doi.org/10.1016/j.conbuildmat.2020.119222

UNEP-SBCI. Buildings and Climate Change, Summary for Decision-Makers, Sustainable Buildings and Climate Initiative, Paris. 2009.

Wargocki P, Wyon D P. Providing better thermal and air quality conditions in school classrooms would be cost-effective. Building and Environment. 2013; 59: 581-589. https://doi.org/10.1016/j.buildenv.2012.10.007

Wolkoff P. Indoor air humidity, air quality, and health – An overview. International Journal of Hygiene and Environmental Health. 2018; 221: 376-90. DOI: 10.1016/j.ijheh.2018.01.015

Woods J, Winkler J, Christensen D. Evaluation of the effective moisture penetration depth model for estimating moisture buffering in buildings. United States. 2013. Web. https://doi.org/10.2172/1067948

Zhang M, Qin M, Chen Z. Moisture Buffer Effect and its Impact on Indoor Environment. Procedia Engineering. 2017a; 205:1123-1129, https://doi.org/10.1016/j.proeng.2017.10.417

Zhang M, Qin M, Rode C, Chen Z. Moisture buffering phenomenon and its impact on building energy consumption. Applied Thermal Engineering. 2017b; 124: 337-345. https://doi.org/10.1016/j.applthermaleng.2017.05.173